Type of contribution:
Editorial
▶ Research Paper
Case Study
Review Paper
Scientific Data
Report of Tech. Application

mesi
e-issn. 2798-5245

Mechanical Engineering
for Society and Industry
Vol. 6, No. 2 (2026) pp 317-324
https://doi.org/10.31603/mesi.14467

Finite element analysis of L4-S1 intervertebral disc stress during ruku' posture in islamic prayer movements

Ojo Kurdi[1*], Kusuma Febriyanto[1,2], Hasyid Ahmad Wicaksono[1,2], Tri Indah Winarni[2,3,4], Jamari[1,2]

[1] Department of Mechanical Engineering, Diponegoro University, Semarang 50275, **Indonesia**
[2] Undip Biomechanics Engineering & Research Centre (UBM-ERC), Diponegoro University, Semarang 50275, **Indonesia**
[3] Department of Anatomy, Diponegoro University, Semarang 50275, **Indonesia**
[4] Center for Biomedical Research (CEBIOR), Diponegoro University, Semarang 50275, **Indonesia**
✉ ojokurdi@ft.undip.ac.id

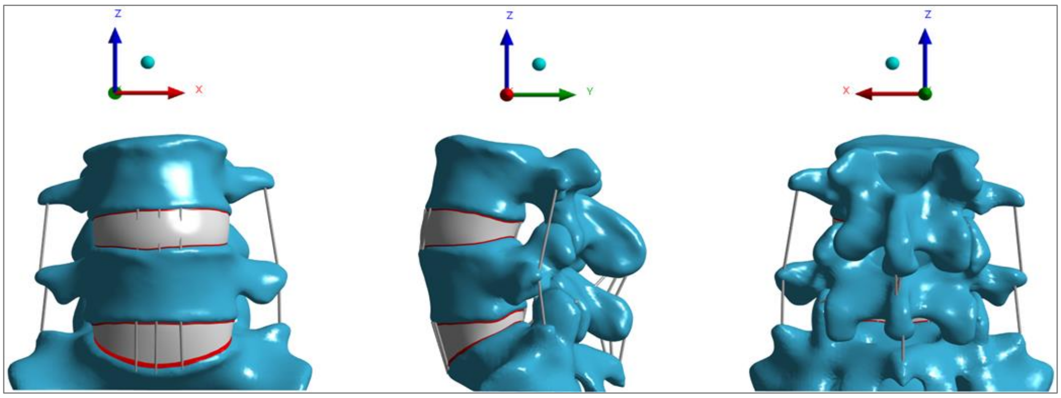

Highlights:

- CT-based FEM simulated ruku' flexion from 0° to 90°.
- Lumbar disc stress increased markedly with flexion angle.
- L5/S1 showed the highest stress in the anterior disc.
- Repeated ruku' may raise biomechanical risk at L5/S1.

Abstract

Bowing movement (ruku') in Islamic prayer requires repeated spinal flexion, which may impose mechanical stress on the spinal structures, particularly in lumbar region. This risk is potentially aggravated in individuals with spinal disorders such as disc degeneration or Hernia Nucleus Pulposus (HNP). Although ruku' posture is a routine daily activity among Muslims, biomechanical investigations into stress distribution during this posture remain limited. This study used finite element model (FEM) to examine von Mises stress distribution in intervertebral disc (IVD) at L4/L5 and L5/S1 levels during flexion movements from 0° to 90°. The geometric model was generated from a CT scan of a 55-year-old male patient. The simulation was conducted under an axial load of 500 N, which was resolved in accordance with the flexion angle's direction. The spinal structure was designed to include the cortical bone, cancellous bone, annulus fibrosus (AF), nucleus pulposus (NP), and related ligaments. The results showed that an increase in the flexion angle led to a substantial accumulation of stress, specifically inside AF and NP. L5/S1 segment demonstrated the greatest stress levels, with distribution mostly focused in the anterior portion of the disc. The highest stress in L5/S1 AF escalated over five times at 90° flexion relative to the upright posture. This pattern indicates a possible posterior displacement of NP, which may theoretically increase the biomechanical risk factors associated with disc herniation over time. Repetitive and intense bowing movements (ruku') can exert significant mechanical stress on the lower lumbar spine, specifically at L5/S1 segment. These results underscore the significance of biomechanical comprehension in religious activities and provide a foundational numerical framework to inform future musculoskeletal investigations regarding postural safety.

Keywords: FEM; Ruku'; IVD; von Mises stress; HNP

Article info
Submitted:
2025-08-04
Revised:
2026-07-01
Accepted:
2026-07-13

Publisher
Universitas Muhammadiyah Magelang

1. Introduction

Human spine is essential for structural support, flexibility, and safeguarding the spinal cord. A significant component is lumbar vertebrae, which consists of cortical bone, cancellous bone, intervertebral disc (IVD), endplate, and ligaments [1]. Lumbar spine is specifically prone to health issues, specifically Hernia Nucleus Pulposus (HNP) [2], a disease characterized by the protrusion of nucleus pulposus (NP) into IVD, resulting in injury to annulus fibrosus (AF) [3]. It is a prevalent cause of lower back pain, affecting about 1% to 3% of the global population each year, predominantly in those aged 30 to 50 years [4].

Numerous factors contribute to the onset of HNP, including degenerative alterations, repetitive strain, and trauma. Repetitive flexion movements can place significant mechanical demands on AF [5]. A particularly frequent flexion activity is ruku' posture in Islamic prayer, characterized by forward bending of lumbar spine. Although ruku' is generally a safe and routine movement, improper posture or excessive repetitive loading in individuals with pre-existing spinal vulnerabilities might theoretically alter load distribution, potentially increasing biomechanical risk factors associated with disc degeneration [6]. During spinal flexion, tension typically accumulates in specific regions of IVD [7], but the exact internal stress distribution during the specific angular progressions of ruku' remains underexplored.

Yamamoto *et al*. performed an in vitro experiment in biomechanical tests of lumbar spine to assess range of motion (ROM) for the spinal column [8]. However, the study was confined to range-of-motion measurements and excluded stress analysis, specifically during ruku' movement. Irianto *et al*. assessed alterations in prayer movements among post-operative Adolescent Idiopathic Scoliosis (AIS) patients by examining motion quality and ROM through video-based motion analysis [9]. Although the study concentrated on prayer movements, it was restricted to ROM observation and did not incorporate musculoskeletal modeling or biomechanical stress analysis. Furthermore, Azari *et al*. examined load-sharing estimation in L4/L5 segment during flexion using a musculoskeletal model and finite element analysis [10]. Despite the significant results, this study was confined to a singular segment (L4/L5), while stress distribution in additional lumbar segments is significant during flexion motions. The results also predominantly emphasized total force and intradiscal pressure (IDP), rather than extensive stress mapping.

Computational approaches, including finite element model (FEM), have been extensively employed alongside experimental and observational techniques for comprehensive biomechanical characterization of spine. FEM facilitates comprehensive analysis of stress and strain distributions in lumbar spine across many situations, yielding significant insights into the mechanical properties of spinal elements [11]. This approach enables the simulation of diverse clinical states, including disc degeneration, scoliosis, and osteoporosis [12]. Previous studies have used FEM to assess the impact on ROM, specifically in flexion movements [10], [13], [14], [15]. However, studies particularly investigating the effects of spinal flexion during ruku' posture in Islamic prayer on IVD remain lacking.

Although numerous studies have used FEM to investigate lumbar flexion [10], [13], [14], [15], literature specifically mapping the internal stress distribution of IVD during the precise angular progressions of ruku' posture remains limited. Therefore, this study aimed to address the gap by exclusively evaluating L4/L5 and L5/S1 segments, which are biomechanically recognized as the primary load-bearing regions and the most susceptible to herniation under extreme flexion. To simulate physiological spinal compression during the posture, a constant 500 N vertical compressive load was applied, which approximates the upper body weight of an average adult male. By varying the angle of the load from 0° to 90°, this study provides a focused biomechanical insight into stress concentrations in AF and NP during prayer.

2. Material and Methods

2.1. Data Collection

Patient-specific CT scan data are essential for accurate lumbar spine modeling. For this study, data were obtained from a 55-year-old male subject (height: 168 cm) who has no antecedent history of bone fractures or trauma. Spine Surgery Department of Dr. Kariadi General Hospital in Semarang provided CT scan data. Ethical approval for this study was granted by the Ethics Committee (Approval No. 108/EC/KEPK/fk-UNDIP/IV/2022), according to institutional and national guidelines.

Table 1. Material properties of FEM

Structure	Elastic Modulus (MPa)	Poisson's Ratio
Cortical bone	12000	0.3
Cancellous bone	100	0.2
Annulus fibrosus	4.2	0.45
Nucleus pulposus	1	0.5
Endplate	2000	0.2
Anterior Longitudinal Ligament	7.8	0.3
Posterior Longitudinal Ligament	10	0.3
Supraspinous Ligament	8	0.3
Interspinous Ligament	8	0.3
Ligamentum Flavum	10	0.3
Intertransverse Ligament	10	0.3
Capsular Ligament	15	0.3

The mechanical properties integrated into the body model for the simulation were sourced from previous studies. The material incorporated into the model pertains to lumbar vertebra, with the characteristics cited from the study by Zewen *et al*. [14], as presented in **Table 1**.

2.2. Finite Element Modelling

CT scan data were processed to identify boundaries using Mimics 21.0 (Materialise Inc., Leuven, Belgium) and subsequently transformed into a geometric model. Geomagic Studio 2021 (Geomagic Inc., Research Triangle Park, NC, United States) was used to import the spinal model as well as to enhance and smooth the shape. SolidWorks 2023 SP 0.1 (Dassault Systèmes Inc., France) was employed to model IVD and endplates in the reconstruction process. FEM was created using ANSYS Workbench (Ansys Inc., Canonsburg, PA, United States).

L4–S1 FEM includes the cortical bone, cancellous bone, endplates, AF, NP, and various principal spinal ligaments, including anterior longitudinal ligament (ALL), posterior longitudinal ligament (PLL), supraspinous ligament (SSL), interspinous ligament (ISL), ligamentum flavum (FL), intertransverse ligament (IL), and capsular ligament (CL). Spinal ligaments anchor spine, specifically during extensive motions, and aid muscles in preserving the alignment of spinal canal [16]. The ligaments biomechanical qualities were designed to withstand tensile forces, allowing elongation and reverting to the former form without injury under typical physiological settings [17]. Consequently, the principal ligaments in this investigation were represented as tension-only components. In FEM, all articulations between IVD, endplates, and vertebral bodies were defined using fully bonded contact formulations to simulate the natural physiological adherence. A 3D tetrahedral element formulation was used for meshing the complex geometries of the vertebrae and disc. **Figure 1** shows L4–S1 FEM that includes the ligaments. The endplate and cortical bone thickness were established at 0.6 mm [15]. In this FEM, NP constitutes 40% of IVD volume [18].

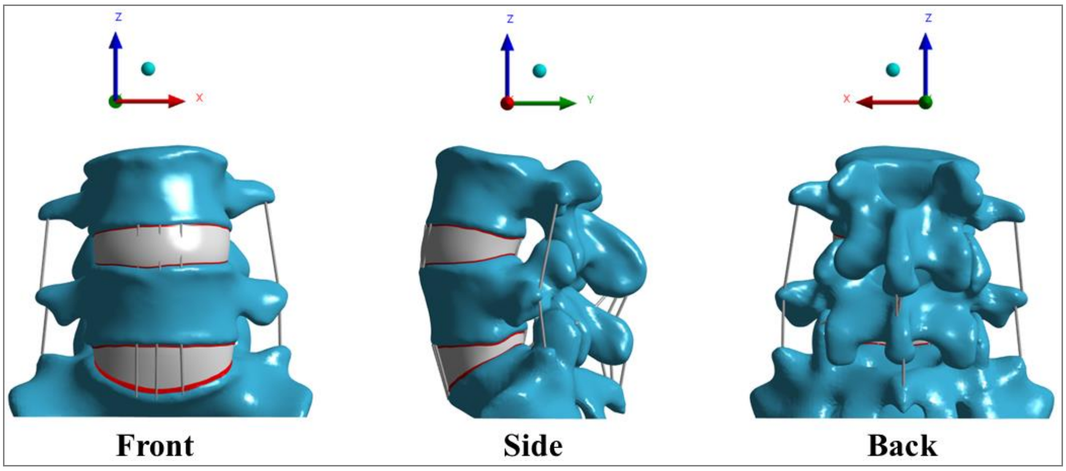

Figure 1. Three-dimensional model of L4-S1 segments including ligament structures. The model is presented from the front, side, and back views. The ligaments are represented as tensioned connectors between the vertebrae to simulate anatomical positioning

2.3. Boundary and Loading Condition

Table 2. Experimental matrix of the 3×3 factorial design

Degree of flexion (°)	Fx (N)	Fy (N)
0	0	500
15	129.5	483
30	250	433
45	353.5	353.5
60	433	250
75	483	129.5
90	500	0

Figure 2 shows the incremental lumbar flexion angles (0°–90°) applied in the finite element simulations to replicate spinal motion during ruku' movement. The inferior surface of S1 vertebra was fully constrained. To represent the physiological compression experienced by the lower back, a vertical compressive load of 500 N was applied, which approximates the weight of the upper body for an average adult male. This load was decomposed into

horizontal (Fx) and vertical (Fy) components based on the specified flexion angle, as presented in **Table 2**.

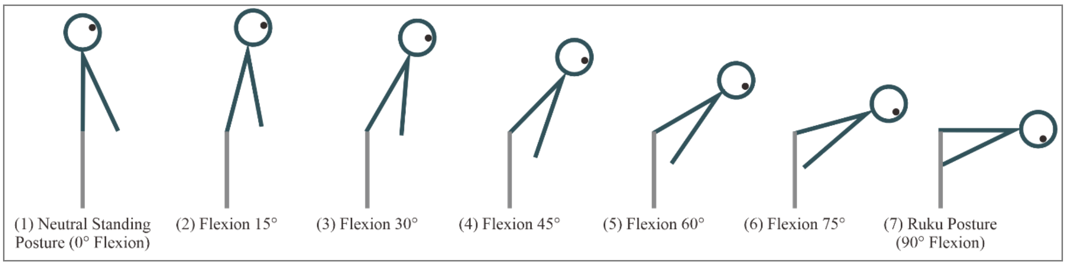

Figure 2. Schematic of lumbar flexion angles (0°–90°) used in FEM to simulate ruku' posture during prayer

3. Results and Discussion

3.1. Process of Mesh Generation

A mesh convergence study is essential to ensure the reliability of numerical simulations by selecting an optimal mesh resolution that produces stable results without excessive computational cost [19]. In this analysis, a 500 N axial load was applied to the superior surface of L4 vertebra. Maximum deformation was selected as the convergence criterion because it is an established and reliable indicator of overall structural stiffness and stability in solid mechanics.

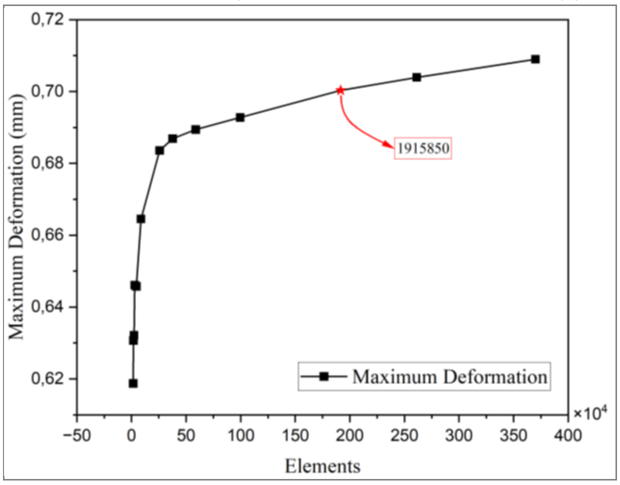

Figure 3. Mesh convergence study showing the relationship between element size and maximum deformation. The red marker indicates the selected mesh size used for subsequent simulations, which balances computational efficiency and solution accuracy

The element size was systematically reduced from 8 mm down to 0.6 mm. The convergence graph (**Figure 3**) demonstrates an increasing trend in maximum deformation as the number of elements increases. However, the solution stabilized significantly upon reaching an element size of 1 mm (1,915,850 elements), yielding a maximum deformation of approximately 0.70 mm. Refining the mesh further to 0.6 mm produced a deformation deviation of only 0.51%. This deviation of less than 1% confirms that the model has successfully achieved convergence [20]. Therefore, to balance computational efficiency and solution accuracy, the 1 mm element size was selected for all subsequent simulations (**Figure 4**).

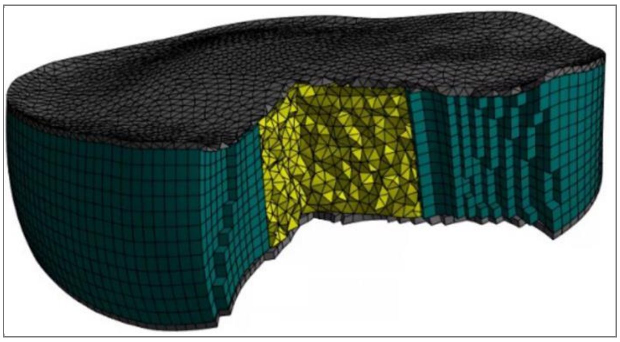

Figure 4. Final meshed model using the optimal mesh configuration (element size = 1 mm)

3.2. Range of Motion

FEM developed in this study was validated by comparing ROM with experimental results reported by Yamamoto, Zewen Shi, Wicaksono, and Zhitao Xiao [8], [14], [21], [22]. A vertical load of 500 N and a torque of 10 Nm were applied to L4 vertebra to simulate body weight and various loading conditions on lumbar spine [14]. The torque was applied along the axis to induce flexion, extension, lateral bending, and axial rotation. ROM results of FEM fell in the range of previously reported data [8], [14], [21], [22], as summarized in **Table 3** and **Figure 5**. Specifically, when comparing the present model results to the well-established in vitro experimental data by Yamamoto *et al*. [8], the percentage differences were calculated to be 8.38% for flexion-extension (16.04° vs 14.8°), 10.41% for lateral bending (10.93° vs 12.2°), and 30.27% for axial rotation (4.82° vs 3.7°). Given the inherent geometrical and anatomical variations between subject-specific models and general in vitro specimens, these percentage differences are considered acceptable and demonstrate the biomechanical reliability of the constructed FEM.

Table 3. The dates of ROM were compared with previous studies

Feedstock	Range of Motion (degree)				
	Present study	Wicaksono's study	Zewen Shi's study	Zhitao Xiao's study	Yamamoto's study
Flexion-extension	16.04	11.26	12.19 ± 2.61	14.2	14.8 ± 2.10
Lateral bending	10.93	10.32	11.46 ± 1.53	13.23	12.2 ± 2.25
Axial rotation	4.82	6.04	5.09 ± 1.22	4.23	3.7 ± 1.50

3.3. Von Mises Stress on L4-S1 During Ruku'

The simulation was conducted by applying a static vertical load under predefined boundary conditions, following the reconstruction and addition of anatomical components such as IVD and ligaments. This study aimed to investigate potential pathological conditions, such as HNP. Finite element analysis was performed to evaluate the distribution of von Mises stress in IVD at L4/L5 and L5/S1 segments under varying load angles ranging from 0° to 90°, with increments of 15°.

The stress distribution in IVD is highly sensitive to the applied flexion angle. **Figure 6** shows that at 0°, the stress is comparatively modest and symmetrically distributed. As the flexion angle increases during bowing, the stress intensifies. NP L4/L5 experiences a stress augmentation of 0.05 MPa, equating to around 22.73% of the original value. The maximum stress is observed in ruku' posture during 75° of flexion. This signifies that NP L4/L5 experiences incremental tension rather than severe stress during flexion.

NP L5/S1 showed a total rise of 96.77%, or twofold, from 0.31 MPa to 0.61 MPa when the flexion angle transitioned from 0° to 90° (**Figure 7**), with peak stress occurring at 60°. In AF L4/L5, the stress escalated nearly thrice (167.65%), rising from 0.68 MPa at 0° flexion to 1.82 MPa at 90° flexion. Simultaneously, the stress on AF L5/S1 escalates over fivefold (399.14%), rising from 1.16 MPa at 0° to 5.79 MPa at 90°.

Figure 7 and **Figure 8** show that the highest von Mises stress is concentrated in the anterior region of IVD. From a biomechanical and load transfer perspective, this occurs because forward flexion causes the anterior margins of the vertebral bodies to approximate, directly compressing the anterior AF while simultaneously inducing tension in the posterior region [23], [24]. This anterior compressive loading shifts the intradiscal pressure, which, over time and under repetitive excessive strain, could theoretically influence posterior displacement of NP [25].

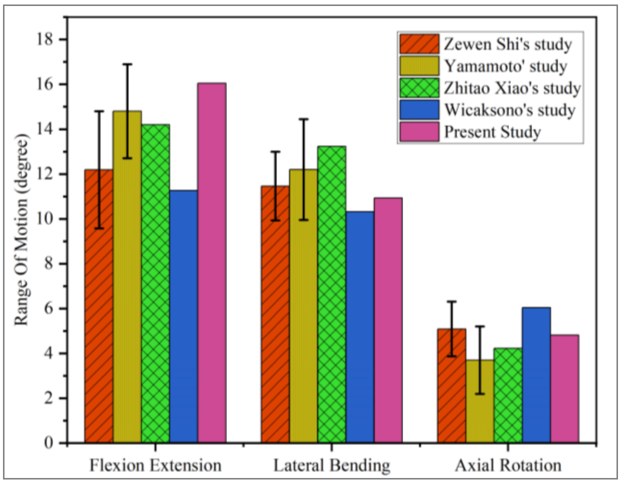

Figure 5. ROM comparison between the present FEM and previous studies, showing consistent results across all motion types

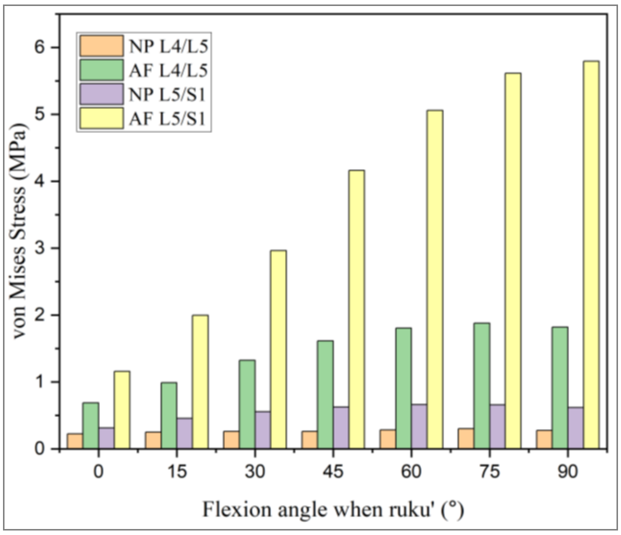

Figure 6. Distribution of von Mises stress in NP and AF of L4/L5 and L5/S1 IVD during various flexion angles representative of ruku' posture

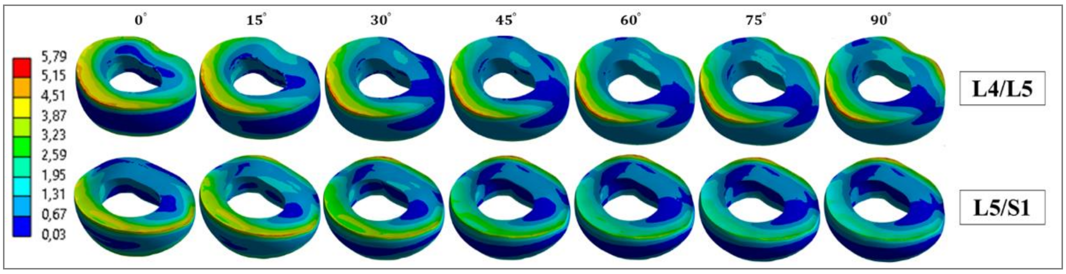

Figure 7. Von Mises stress distribution in AF of L4/L5 (top) and L5/S1 (bottom) during flexion angles from 0° to 90°

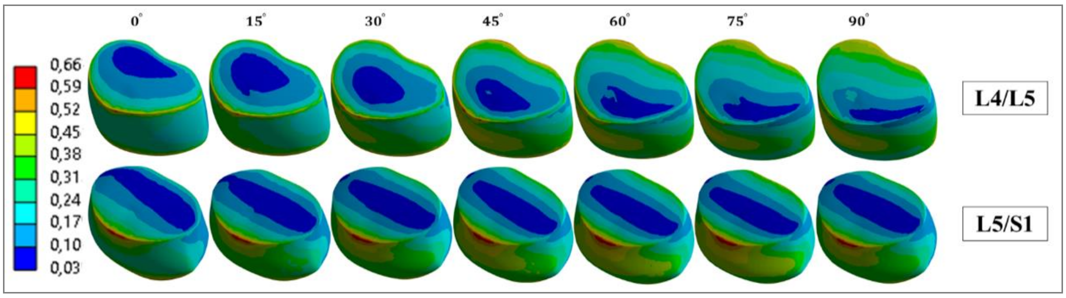

Figure 8. Von Mises distribution in NP of L4/L5 (top) and L5/S1 (bottom) during flexion angles from 0° to 90°

L5/S1 segment experiences substantially higher stress compared to L4/L5 at all flexion angles [22]. This is consistent with spinal anatomy, as L5/S1 segment is located at the transitional base of the spine. It must bear the highest cumulative axial load from the upper body and accommodate the steepest lumbosacral shear angle during forward bending. Although the peak stress in L5/S1 AF reached 5.79 MPa at 90° flexion, this value remains below the ultimate tensile failure stress of healthy AF tissue, which ranges between 10 MPa and 15 MPa. This shows that although ruku' imposes significant localized stress, it generally remains within the physiological tolerance of healthy tissues for brief, dynamic movements [26]. However, the marked stress escalation nearing 90° underscores the biomechanical importance of maintaining proper alignment during ruku' posture to prevent potential stress overload, particularly in individuals with compromised spinal integrity.

4. Study Limitations

This study has several limitations that are important for interpreting the results. First, the model relies on data from a single 55-year-old male subject. This implies that the results cannot be directly generalized to broader populations with different ages, sexes, or body sizes. Second, the material properties of IVD were simplified. NP and AF were modeled as homogeneous, linearly elastic materials, which do not fully capture the anisotropic, fiber-reinforced structure of annulus or viscoelastic behavior of nucleus. Third, the model validation was limited to ROM comparisons. Future studies should incorporate validations against intradiscal pressure or experimental disc stress measurements. Fourth, the mesh convergence study relied on maximum deformation due to computational resource constraints, while demonstrating stress convergence would yield more robust localized stress predictions. Furthermore, the loading condition used a constant 500 N load where only the force direction changed. In reality, spinal loading during ruku' is a dynamic process influenced by shifting body weight distribution, dynamic muscle forces, and changing moment arms that were not accounted for in this static simulation. Finally, because no damage criteria or annulus rupture models were included, statements regarding herniation risk remain theoretical interpretations based on stress concentrations rather than direct simulations of tissue failure. Fifth, no comprehensive sensitivity analysis was performed regarding the assumed material properties or ligament stiffnesses, which could potentially influence the specific magnitude of the predicted stresses. Sixth, this study is entirely numerical and lacks direct experimental verification, such as in vitro stress measurements. Therefore, the results should be interpreted as theoretical predictions. Ruku' posture was modeled primarily by changing the load vector on a static spinal geometry. In reality, the movement involves substantial changes in spinal alignment, pelvic rotation, and trunk inclination, suggesting this static representation does not fully capture the complex kinematic load transfer mechanisms of the actual prayer movement.

5. Conclusions

In conclusion, this study used finite element analysis to assess the stress distribution in IVD at L4/L5 and L5/S1 segments during ruku’ posture in Salat. The simulation results indicated that flexion movements significantly affect stress accumulation, specifically in AF and NP. At elevated flexion angles, particularly between 60° and 90°, a significant increase in von Mises stress was observed in both disc segments, with the greatest concentration occurring at L5/S1. The tension was primarily concentrated in the anterior section of the disc, indicating a possible posterior displacement of NP. The condition may increase the risk of herniation, specifically in the posterior AF, which is prone to deterioration. This study establishes a fundamental numerical basis for understanding load distribution during religious activities, which can inform future dynamic musculoskeletal and experimental investigations on postural safety.

Authors' Declaration

Authors' contributions and responsibilities - Ojo Kurdi, Kusuma Febriyanto, Hasyid Ahmad Wicaksono, Tri Indah Winarni, and Jamari contributed to the conception and design of the study, methodology, data analysis, interpretation of results, and preparation and revision of the manuscript. All authors read and approved the final version of the manuscript.

Funding – No external funding was received for this study.

Availability of data and materials - The data supporting the findings of this study are available from the corresponding author upon reasonable request.

Competing interests - The authors declare no competing interests.

Generative AI statement - The authors declare that no generative AI tools were used in the preparation of this paper.

Additional information – The authors have no additional information to disclose.

References

[1] R. Aiyer, *An overview on the anatomy of the spine*. 2023. doi: 10.1016/B978-0-323-87751-0.00010-X.

[2] Y. Kitagawa *et al.*, "Minimally invasive and simultaneous removal of herniated intracanal and extracanal lumbar nucleus pulposus with a percutaneous spinal endoscope.," *Asian journal of endoscopic surgery*, vol. 5, no. 4, pp. 183 – 186, 2012, doi: 10.1111/j.1758-5910.2012.00144.x.

[3] A. D. Pratama and M. E. Salam, "The Effectiveness of Core Stability Exercise to Improve Functional Ability in A Lumbar Herniated Nucleus Pulposus Patient: A Case Study," *Physical Therapy Journal of Indonesia*, vol. 2, no. 2, pp. 61 – 66, 2021, doi: 10.51559/ptji.v2i2.24.

[4] A. S. Zhang *et al.*, "Lumbar Disc Herniation: Diagnosis and Management," *American Journal of Medicine*, vol. 136, no. 7, pp. 645 – 651, 2023, doi: 10.1016/j.amjmed.2023.03.024.

[5] C. Balkovec and S. McGill, "Extent of nucleus pulposus migration in the annulus of porcine intervertebral discs exposed to cyclic flexion only versus cyclic flexion and extension," *Clinical Biomechanics*, vol. 27, no. 8, pp. 766 – 770, 2012, doi: 10.1016/j.clinbiomech.2012.05.006.

[6] J. A. Hassan, S. Milosavljevic, and A. Carman, "Can postural modification reduce kinetic and kinematic loading during the bowing postures of Islamic prayer?," *Ergonomics*, vol. 53, no. 12, pp. 1446–1454, 2010, doi: 10.1080/00140139.2010.532881.

[7] T. T. Dao, "Enhanced Musculoskeletal Modeling for Prediction of Intervertebral Disc Stress Within Annulus Fibrosus and Nucleus Pulposus Regions During Flexion Movement," *Journal of Medical and Biological Engineering*, vol. 36, no. 4, pp. 583 – 593, 2016, doi: 10.1007/s40846-016-0156-6.

[8] I. Yamamoto, M. M. Panjabi, T. Crisco, and T. Oxland, "Three-dimensional movements of the whole lumbar spine and lumbosacral joint.," *Spine*, vol. 14, no. 11, pp. 1256–1260, Nov. 1989, doi: 10.1097/00007632-198911000-00020.

[9] K. A. Irianto, N. R. Firas, C. G. S. Binti, D. Tinduh, Y. M. Sakti, and B. De Vega, "The impact of spinal fusion of adolescent idiopathic scoliosis in Salah (Islamic Prayer) movement: a case-control study," *F1000Research*, vol. 11, p. 1054, 2022, doi: 10.12688/f1000research.124255.2.

[10] F. Azari, N. Arjmand, A. Shirazi-Adl, and T. Rahimi-Moghaddam, "A combined passive and active musculoskeletal model study to estimate L4-L5 load sharing," *Journal of Biomechanics*, vol. 70, pp. 157–165, 2018, doi: 10.1016/j.jbiomech.2017.04.026.

[11] Q. Liu, J. Zhang, S.-C. Sun, and F. Wang, "Application of finite element method in spinal biomechanics," *Zhongguo gu shang = China journal of orthopaedics and traumatology*, vol. 30, no. 2, pp. 190 – 194, 2017, doi: 10.3969/j.issn.1003-0034.2017.02.020.

[12] B. Khuyagbaatar, K. Kim, and Y. H. Kim, "Recent Developments in Finite Element Analysis of the Lumbar Spine," *International Journal of Precision Engineering and Manufacturing*, vol. 25,

no. 2, pp. 487 – 496, 2024, doi: 10.1007/s12541-023-00866-9.

[13] P. G. Cho, S. J. Yoon, D. A. Shin, and M. C. Chang, "Finite Element Analysis of Stress Distribution and Range of Motion in Discogenic Back Pain," *Neurospine*, vol. 21, no. 2, pp. 536–543, 2024, doi: 10.14245/ns.2347216.608.

[14] Z. Shi *et al.*, "The biomechanical effect on the adjacent L4/L5 segment of S1 superior facet arthroplasty: a finite element analysis for the male spine," *Journal of Orthopaedic Surgery and Research*, vol. 16, no. 1, pp. 1–9, 2021, doi: 10.1186/s13018-021-02540-0.

[15] R. Liu, T. He, X. Wu, W. Tan, Z. Yan, and Y. Deng, "Biomechanical response of decompression alone in lower grade lumbar degenerative spondylolisthesis--A finite element analysis," *Journal of Orthopaedic Surgery and Research*, vol. 19, no. 1, pp. 1–11, 2024, doi: 10.1186/s13018-024-04681-4.

[16] M. K. Cleveland and R. S. Tubbs, *The Ligaments of the Lumbar Spine*. 2019. doi: 10.1016/B978-0-323-67376-1.00009-4.

[17] J. Yao, Z. Lian, B. Yang, and Y. Fan, *Biomechanics of ligaments*. 2020. doi: 10.1007/978-981-15-3159-0_3.

[18] Z. Xu, Q. Zheng, L. Zhang, R. Chen, Z. Li, and W. Xu, "Biomechanical evaluation of different oblique lumbar interbody fusion constructs: a finite element analysis," *BMC Musculoskeletal Disorders*, vol. 25, no. 1, pp. 1–16, 2024, doi: 10.1186/s12891-024-07204-8.

[19] S. Kikale, A. Katkati, A. Kulkarni, A. Mache, A. Deshpande, and S. Shinde, "Mesh Convergence Study on Side Bracket using Hex-dominant and Tetrahedron-dominant Mesh," *International Journal of Vehicle Structures and Systems*, vol. 16, no. 6, pp. 837 – 840, 2024, doi: 10.4273/ijvss.16.6.05.

[20] E. M. Yusup, H. Azahari, S. Saiful, F. Mansor, M. N. H. Mat, and B. A. Jabbar, "A Mesh Convergence Study for 2D Axisymmetric Pipe Wall Thickness," *Journal of Advanced Research in Micro and Nano Engineering*, vol. 23, no. 1, pp. 77–90, 2024, doi: 10.37934/armne.23.1.7790.

[21] H. A. Wicaksono *et al.*, "Analysis of Von Mises stress on Lumbar 4 to Sacral 1 with variation in body mass index," *Jurnal Tribologi*, vol. 45, no. November 2024, pp. 174–184, 2025.

[22] Z. Xiao, L. Wang, H. Gong, and D. Zhu, "Biomechanical evaluation of three surgical scenarios of posterior lumbar interbody fusion by finite element analysis.," *Biomedical engineering online*, vol. 11, p. 31, Jun. 2012, doi: 10.1186/1475-925X-11-31.

[23] A. Tsantrizos, K. Ito, M. Aebi, and T. Steffen, "Internal Strains in Healthy and Degenerated Lumbar Intervertebral Discs," *Spine*, vol. 30, no. 19, pp. 2129–2137, Oct. 2005, doi: 10.1097/01.brs.0000181052.56604.30.

[24] O. Ardatov *et al.*, "Modeling the Effect of Annulus Fibrosus Stiffness on the Stressed State of a Vertebral L1 Body and Nucleus Pulposus," *Bioengineering*, vol. 11, no. 4, 2024, doi: 10.3390/bioengineering11040305.

[25] S. N. Zahari, M. J. Abd Latif, and M. R. A. Kadir, "The influence of preload application for vertebra segment in finite element modelling," *IECBES 2014, Conference Proceedings - 2014 IEEE Conference on Biomedical Engineering and Sciences: "Miri, Where Engineering in Medicine and Biology and Humanity Meet,"* no. December, pp. 198–203, 2014, doi: 10.1109/IECBES.2014.7047485.

[26] X. Ning, J. Zhou, B. Dai, and M. Jaridi, "The assessment of material handling strategies in dealing with sudden loading: The effects of load handling position on trunk biomechanics," *Applied Ergonomics*, vol. 45, no. 6, pp. 1399 – 1405, 2014, doi: 10.1016/j.apergo.2014.03.008.